

Physics with jets at LHCb

Roger Barlow^{*†}

University of Huddersfield (GB)

E-mail: roger.barlow@cern.ch

LHCb has a unique capability to separate beauty and charm jets. We present recent results on jet tagging performance, W+b,c jets and the observation of the top quark in the forward acceptance at the LHC.

*The European Physical Society Conference on High Energy Physics
22-29 July 2015
Vienna, Austria*

^{*}Speaker.

[†]Representing the LHCb collaboration.

1. The LHCb experiment

The LHCb detector was built primarily for studies of CP violation in the B mesons produced copiously in high energy pp collisions. It covers the forward region of the pp collisions, with a layout shown in figure 1: the beams interact in the Vertex Locator (VELO) and outgoing tracks are analysed by a 1.1T magnet, instrumented by tracking chambers, Ring Imaging Cherenkov (RICH) detectors for particle identification, an electromagnetic calorimeter which detects photons and identifies electrons, a hadronic calorimeter and muon chambers [1].

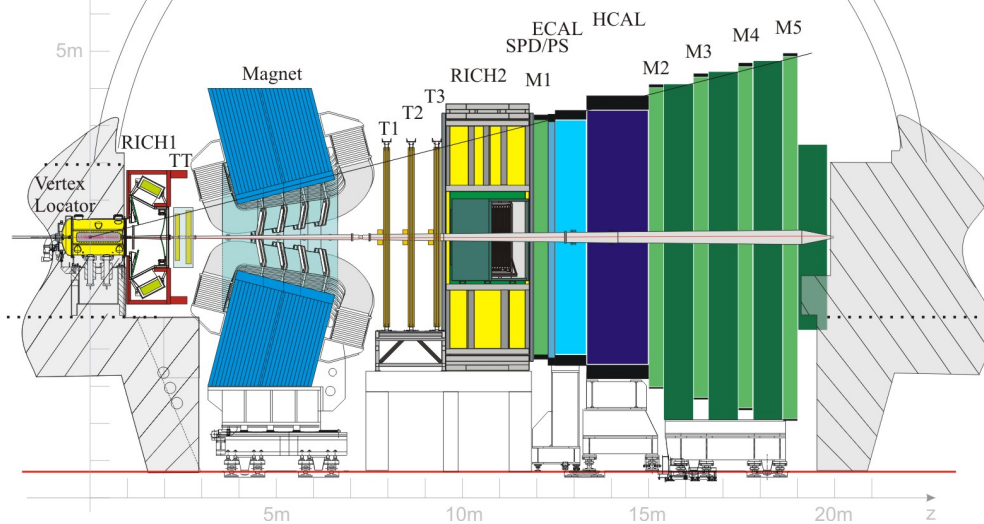


Figure 1: The LHCb detector

The detector thus provides

- Coverage of the forward region, $2 < \eta < 5$
- Excellent tracking with $\frac{\sigma_p}{p} \approx 0.5\%$
- Outstanding vertexing with precision $\sim 0.01 - 0.05 \text{ mm}$ in xy and $\sim 0.1 - 0.3 \text{ mm}$ in z
- Superb $K/\pi/p$ separation from the RICH detectors
- Good μ ID, and a μ trigger
- An inclusive B trigger, with efficiency $\sim 30 - 45\%$ for $p_T > 15 \text{ GeV}$

The experiment accumulated 1 fb^{-1} at 7 TeV in 2011, 2 fb^{-1} at 8 TeV in 2012. This has produced many results: the collaboration has just published its 250th paper. It is, however, fair to say that most of these have explored the power of the detector to examine the decays of specific hadrons, through particle identification and precise mass measurements.

However LHCb can also be used for jet studies, probing physics at the parton level. This note explores this area: the techniques for jet finding and for b and c jet identification are introduced. These are used to measure the $b\bar{b}$ asymmetry, and then the properties of vector boson (Z and W) production in association with jets, before finally presenting the observation of top quark production in the forward region.

2. Jet Techniques

2.1 Jet identification: algorithms

Jets are formed by clustering with with standard anti- k_T algorithm, with $R = 0.5$.

Jet energy is found using the particle flow algorithm (PFA). The validity of this technique can be checked by selecting a sample of events in which a Z and a jet are produced at high P_T . Z particles can be cleanly identified in their $\mu^+\mu^-$ decays and their transverse momentum is well measured. The observed ratio P_T^{jet}/P_T^Z peaks at 1 and there is good agreement between the data and the simulations. Our jet energy scale is well calibrated and unproblematic.

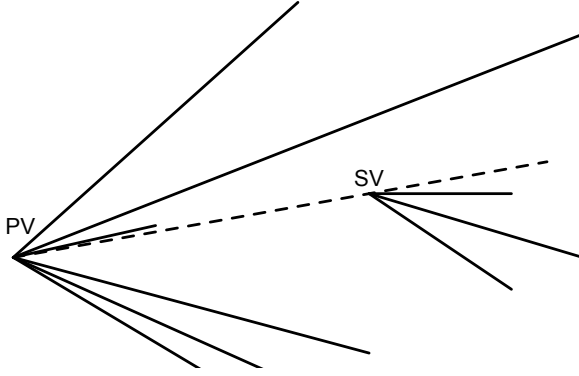


Figure 2: Schematic showing the reconstruction of a primary and secondary vertex from charged tracks in the VELO

Primary (PV) and secondary (SV) vertices are reconstructed from the measured tracks, as shown in Figure 2. θ is the angle between the reconstructed momentum and the flight direction (having both geometric and kinematic information is a great advantage), and M is the invariant mass of the secondary, constructed from its observed decay products.. A useful derived quantity is

$$M_{corr} = \sqrt{M^2 + p^2 \sin^2 \theta} + p \sin \theta$$

which is the minimum mass of this secondary, including unobserved objects that balance momentum transverse to the flight path.

b and c quark jets are then identified using two separate algorithms. [2]

The **SV tagger** method was developed to be run offline. Tracks are identified as not belonging to any production vertex, if adding them to the vertex would raise the χ^2 of the fit by 16 or more. Pairs of such tracks are taken, and merged to and form a secondary vertex.

Two BDTs are then applied, each with 10 inputs including M , M_{corr} , d_T^{min} , $\frac{p_T(SV)}{p_T^{jet}}$, ΔR , N_{SV} , $N_{SV}(\Delta R < 0.5)$, $Q(SV)$. One BDT has been trained to discriminate light ($udsg$) from heavy (bc) jets, and the other trained to distinguish b from c jets.

The **TOPO method** was developed for the online trigger, and is used only for b jet identification. Two-track SVs are combined to build SVs with up to 4 tracks. The properties are then fed to a single BDT which has been trained to identify b jets.

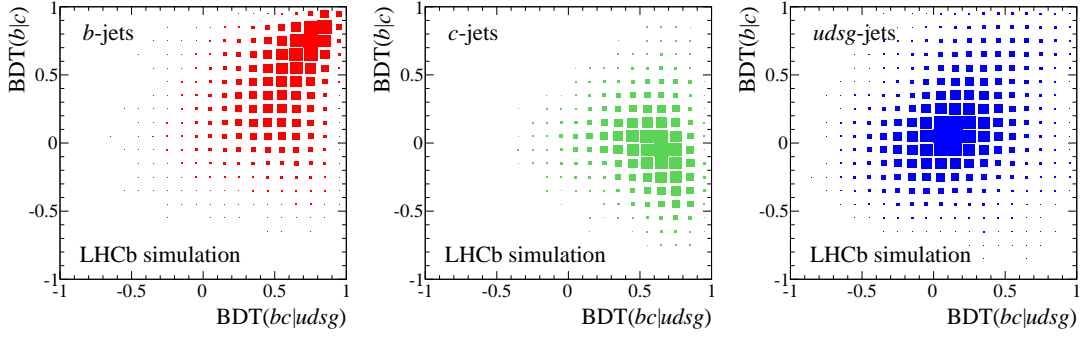


Figure 3: BDT outputs from simulated samples of (a) b -jets (b) c -jets and (c) light jets. The horizontal axis distinguishes heavy from light jets, the vertical axis b from c jets.

2.2 Jet identification: performance

Figure 3 shows the outputs from the two SV tagger BDTs for simulated jet samples. There is good discrimination between heavy and light jets by one BDT, and between b and c by the other. Separation is not perfect, but sufficient for samples of b and c jets to be selected with low background and reasonable efficiency, of order tens of percent: it varies as a function of η and p_T , as can be seen in Figure 4. Many more performance plots are available[2].

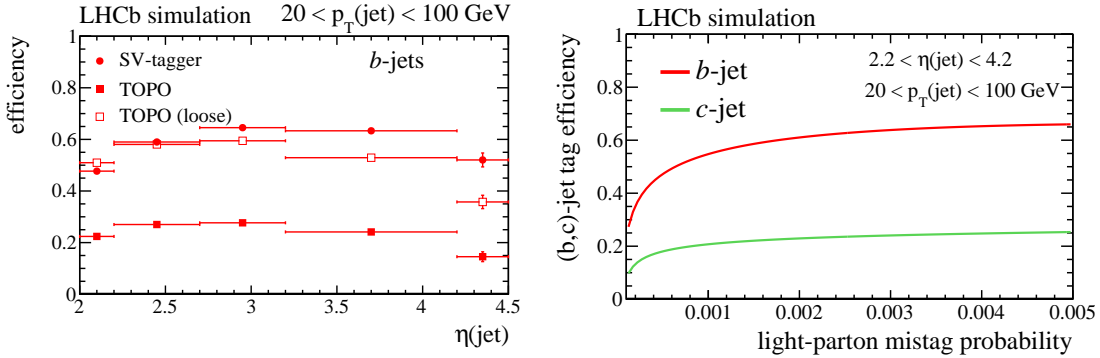


Figure 4: Efficiency and background for b and c jet tagging

The performance of the jet identification can also be evaluated using the data. Two-jet events are selected, with the jets separated by $\Delta\phi > 2.5$.

If the particles in one jet contain a reconstructed B hadron, that tags the second jet as a b jet. A reconstructed D meson tags a possible b or c jet. A μ in the jet also indicates a b or c for the second jet, whereas an isolated μ is a sign of W decay, associated with a light quark or gluon jet. The data are fitted to template distributions, and the fits describe the data well. An example is shown in Figure 5: more can be found in [2].

We use two independent methods for normalisation, with different systematics. One is to use jets with identified muons, which (almost certainly) come from heavy quarks, and for which the efficiency is well known. The second is to estimate the number of secondary vertices from the distribution of the $\Delta\chi^2$ for the highest p_T track in the jet.

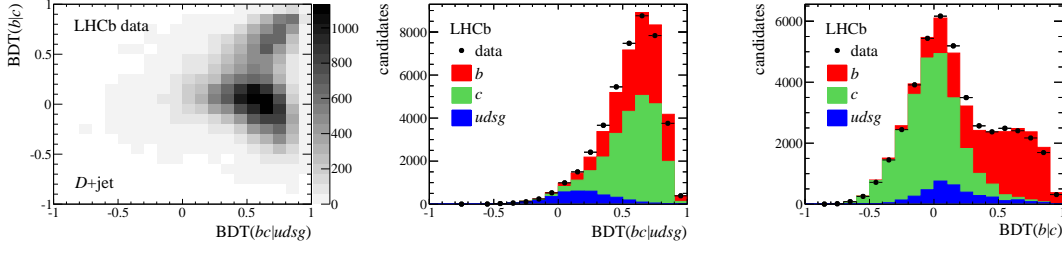


Figure 5: BDT outputs for different D tagged jets, showing the two-dimensional BDT indicators for b versus c and light versus heavy, and the two projections with fitted contributions from the three templates.

Results agree well and show that we have an efficiency of 65% for b jets and 25% for c jets, with the probability of a light ($udsg$) jet being misidentified as heavy of 0.3%, for jets with $p_T > 20\text{GeV}$ and $2.2 < \eta < 4.2$.

3. Measurement of the $b\bar{b}$ asymmetry

The asymmetry is defined as $A_C^{b\bar{b}} = \frac{N_+ - N_-}{N_+ + N_-}$ where N_+ is number of events where $\Delta y = |y_b| - |y_{\bar{b}}| > 0$. As we are in the forward direction, $|y|$ can be replaced by y [3]. A positive asymmetry would mean that b quarks had more energy than \bar{b} quarks, and vice versa. It is hard to imagine how such an effect could arise; it cannot occur at leading order through the $g \rightarrow b\bar{b}$ process, though it can arise at higher orders through the q/\bar{q} asymmetry in pdfs. However it was suggested by the $t\bar{t}$ asymmetry reported by the Tevatron experiments[4].

This analysis was performed using the TOPO tagger twice, once for each b . Using looser cuts for the second jet this gave a joint efficiency of efficiency of 30%, with a mistag probability below 0.1%. for jets in the region $p_T > 2\text{GeV}$, $p > 10\text{GeV}$ The charge of the b was taken from the charge of the muon. The mass of the pair, $M_{b\bar{b}}$ was measured to $\sim 15\%$ The quantity Δy was unfolded using a migration matrix.

$M_{b\bar{b}}$	$A_C^{b\bar{b}} \%$	err(stat)	err(sys)
40 – 75 GeV	0.4	0.4	0.3
75 – 105 GeV	2.0	0.9	0.6
> 105 GeV	1.6	1.7	0.6

Table 1: The $b\bar{b}$ asymmetry and associated errors for regions of $M_{b\bar{b}}$ below, around, and above the Z^0 peak

The measured values and their errors (systematic errors are small, due on large part to the periodic LHCb magnet reversal) are shown in Table 1. Results are consistent with zero. This does not contradict the Tevatron results but does constrain some of the models that have been developed to explain it. A full account of the theoretical implications can be found in Gauld *et al.*[5].

4. $Z + b$ methods and results

To study the production of b jets produced in association with a Z boson, [6], the Z is found by selecting a pair of muons (with $p_T > 20\text{GeV}$, $2.0 < \eta < 4.5$) with $60 < M_{\mu\mu} < 120\text{ GeV}$. The b jets were selected using a loose version of the TOPO algorithm.

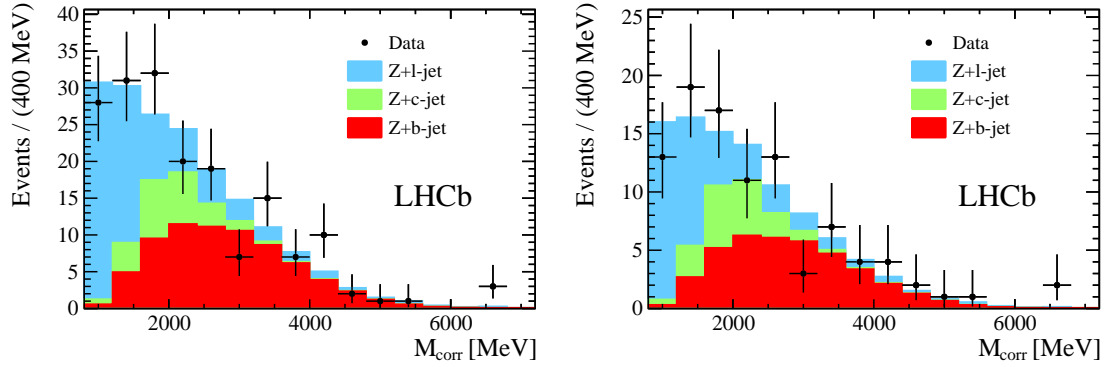


Figure 6: The M_{corr} distributions for selected $Z + jet$ combinations, for $p_T(jet)$ above 10 and 20 GeV

Figure 6 shows the measured distributions of M_{corr} (as defined earlier) with the expected contributions from different processes shown. From these graphs the cross sections for Zb are determined as:

For b jets above 10 GeV: $\sigma(Zb) = 295 \pm 60 \pm 51 \pm 10\text{ fb}$.

For b jets above 20 GeV: $\sigma(Zb) = 128 \pm 36 \pm 22 \pm 5\text{ fb}$.

where the errors shown are statistical, systematic, and from the luminosity determination. These are in good agreement with the predictions of the Standard Model, as shown in Figure 7.

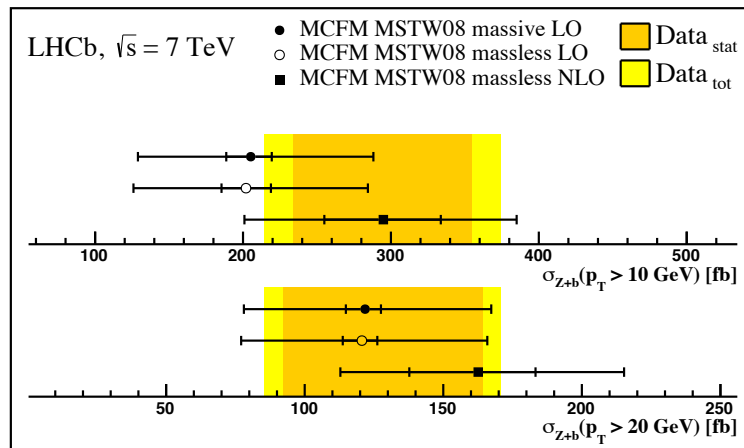


Figure 7: Comparison of the Zb cross sections with Standard Model predictions

5. $W + b, c$ methods and results

$W + jet$ event selection [7], through the decay $W \rightarrow \mu\nu$ is not as simple as Z selection through $Z \rightarrow \mu\mu$ due to the invisible neutrino. They are selected by requiring a high $P_T (> 20 GeV/c)$ muon. A separate high P_T jet (with $\Delta R > 0.5$) is then required.

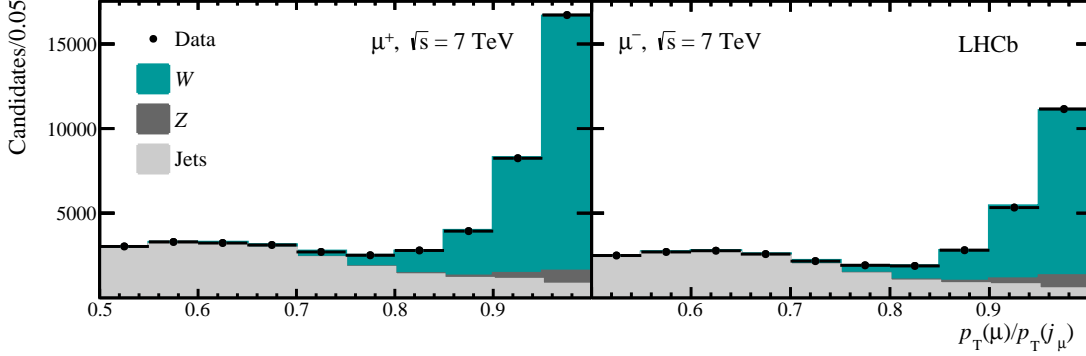


Figure 8: The ratio $p_T(\mu)/p_T(jet)$, for μ^+ and μ^- samples.

The ratio $p_T(\mu)/p_T(\mu jet)$ is a measure of the isolation of the muon, and the W contribution peaks at large values. The distributions are shown in Figure 8 (for the 7 TeV data: the plots for 8 TeV are similar.) Contributions are fitted using templates from data.

The jet flavour is then tagged using the SV technique. Each $p_T(\mu)/p_T(\mu jet)$ bin is fitted separately separately. Figure 9 shows the results for the highest bin.

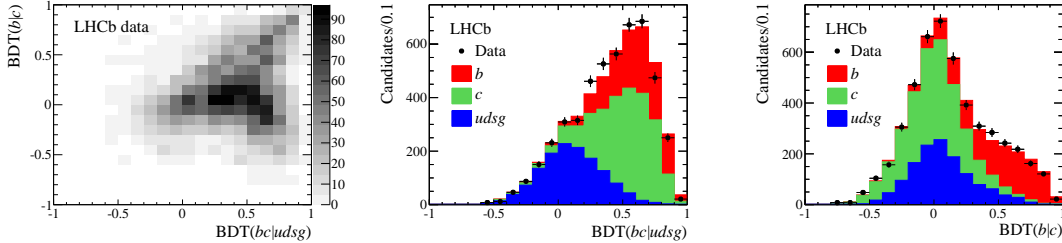


Figure 9: BDT output for the highest $p_T(\mu)/p_T(jet)$ bin.

A matching $Z + jet$ sample is obtained from events with a second muon, $60 < M_{\mu\mu} < 120 GeV$. Taking ratios eliminates many systematic uncertainties. The dominant remaining one are (where applicable) the b, c tag efficiencies , the $p_T(\mu)/p_T(\mu jet)$ templates, and the t quark contribution. Results for the ratios of cross sections and for the asymmetries $A(Wx) = \frac{\sigma(W^+x) - \sigma(W^-x)}{\sigma(W^+x) + \sigma(W^-x)}$ are given in Table 2 and Figure 8.

Results provide no support for any intrinsic b component in proton - but cannot completely rule it out. They do provide useful constraints on the parton pdfs used (we used the CT10 set[8].) In particular, the Wc results constrain s quark pdfs down to $x \sim 10^{-5}$

Figure 10 shows the same numbers graphically.

	7 TeV result	8 TeV result	7 TeV pred	8 TeV pred
$\sigma(Wb)/\sigma(Wj) \times 10^2$	$0.66 \pm 0.13 \pm 0.13$	$0.78 \pm 0.08 \pm 0.16$	$0.74^{+0.17}_{-0.13}$	$0.77^{+0.18}_{-0.13}$
$\sigma(Wc)/\sigma(Wj) \times 10^2$	$5.80 \pm 0.44 \pm 0.75$	$5.62 \pm 0.28 \pm 0.73$	$5.02^{+0.80}_{-0.69}$	$5.31^{+0.87}_{-0.52}$
$\sigma(W^+j)/\sigma(Zj)$	$10.49 \pm 0.28 \pm 0.53$	$9.44 \pm 0.19 \pm 0.47$	$9.90^{+0.28}_{-0.24}$	$9.48^{+0.16}_{-0.33}$
$\sigma(W^-j)/\sigma(Zj)$	$6.61 \pm 0.19 \pm 0.33$	$6.02 \pm 0.13 \pm 0.30$	$5.79^{+0.21}_{-0.18}$	$5.52^{+0.13}_{-0.25}$
$A(Wb)$	$0.51 \pm 0.20 \pm 0.09$	$0.27 \pm 0.13 \pm 0.09$	$0.27^{+0.03}_{-0.03}$	$0.28^{+0.03}_{-0.03}$
$A(Wc)$	$-0.09 \pm 0.08 \pm 0.04$	$-0.01 \pm 0.05 \pm 0.04$	$-0.15^{+0.02}_{-0.04}$	$-0.14^{+0.02}_{-0.03}$

Table 2: Ratios and asymmetries for cross sections for b and c jets produced in association with a W .

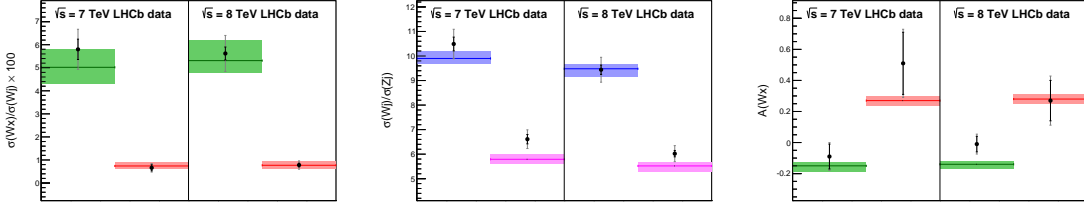


Figure 10: Graphical presentation of the results

6. Top quark production in the forward region

t production in the forward region has not previously observed. Although the properties of the t are, of course, the same, forward t production is thought to occur by a different set of processes from central production: from $q\bar{q}$ and qg rather than gg fusion. At NLO, we expect about 75% $t\bar{t}$ and about 25% t channel single top production.

The measurements will provide useful constraints on the large x gluon pdf, and tests of NNLO calculations. Also charge asymmetries are potentially sensitive to BSM physics.

Event selection is the same as for the Wb channel, but with reduced fiducial region to enhance contribution from $t \rightarrow Wb$: $p_T(\mu) > 25\text{GeV}$ $2.0 < \eta(\mu) < 4.5$

Again, the W is identified from high energy muon from $W \rightarrow \mu\nu$ decay. μ also put into jet (j_μ) by clustering algorithm.

The jet energy correction, of order 10%, is obtained from simulation. It depends on p_T , η , and the number of interactions in the event.

We require $p_T(j_\mu + b) > 20\text{ GeV}$, to suppress background from dijets (which have no neutrinos) Also we use a reduced region in rapidity, $2.2 < \eta(b) < 4.2$, to reduce the variation in efficiency. The transverse momentum of the b jet is required to lie in the region $50 < P_T(b) < 100\text{GeV}/c$, where the upper limit is imposed as the SV tagger performance is not known above this.

Results [9] are shown in Figure 11. The data are incompatible with the expected contribution from Wb production (red) but agree well if the contribution from $W + \text{top}$ is also concluded (turquoise). The result is significant at 5.4σ (using Wilks' theorem for the likelihood difference). Incidentally, a similar analysis for $W + c$ gives good agreement with no t contribution.

The Wt contribution cross section can be found by fitting the data in Figure 11, and the results are given in Table 3.

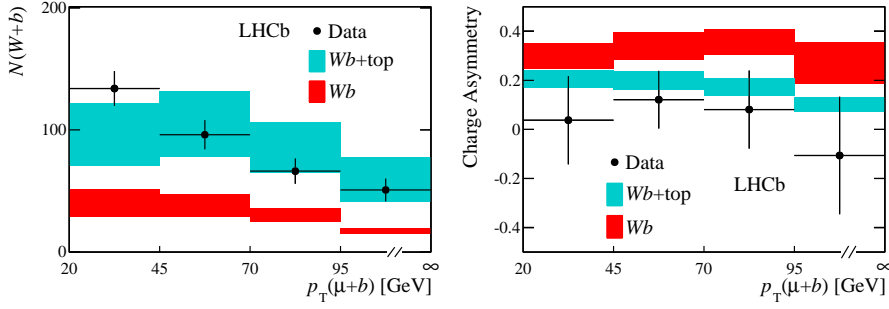


Figure 11: $P_T(\mu + b)$ distribution and asymmetry for selected events

\sqrt{s}	Data	SM prediction
7 TeV	$239 \pm 53 \pm 38$ fb	180^{+51}_{-41} fb
8 TeV	$289 \pm 43 \pm 46$ fb	312^{+83}_{-68} fb

Table 3: Cross section for t production obtained from the fits.

7. Conclusions and outlook

LHCb is a powerful tool to study heavy quark jets. These jets can be combined with lepton identification to study the production and decay properties of W and Z bosons. This has led to many physics results, including the first observation of top quark production in the forward region.

In the forthcoming Run II the higher energies will produce significantly higher cross-sections, by factors of 10 or more, for the various top quark production processes, and a wealth of new results will follow.

References

- [1] A. A. Alves Jr *et al.*, (The LHCb collaboration) *The LHCb detector at the LHC*, JINST **3** S08005 (2008)
- [2] R. Aaj *et al.* (the LHCb collaboration), *Identification of beauty and charm quark jets at LHCb*, JINST **10**(2015) P06013
- [3] R. Aaj *et al.* (the LHCb collaboration), *First Measurement of the Charge Asymmetry in Beauty-Quark Pair Production*, PRL **113** 082003, (2014)
- [4] T. Aaltonen *et al.* (The CDF Collaboration), *Evidence for a Mass Dependent Forward-Backward Asymmetry in Top Quark Pair Production*, Phys. Rev. D **83**, 112003 (2011)
- [5] R. Gauld *et al.*, *Leptonic top-quark asymmetry predictions at LHCb*, Phys Rev **D91** 054029 (12015)
- [6] R. Aaj *et al.* (the LHCb collaboration) *Measurement of the Z + b-jet cross-section in pp collisions at $\sqrt{s} = 7$ TeV in the forward region*, JHEP 2015 064 (2015)
- [7] R. Aaj *et al.* (the LHCb collaboration) *Study of W boson production in association with beauty and charm*, arXiv 1505.04051 (2015)
- [8] H-L Lai *et al.*, *New parton distributions for collider physics*, Phys.Rev.**D82** 074024, (2010)
- [9] R. Aaj *et al.* (the LHCb collaboration) *First observation of top quark production in the forward region*, Phys. Rev. Lett. **115**, 112001 (2015)